



This is a repository copy of *Determination of the thin film structure of zwitterion doped poly(3,4-ethylenedioxythiophene):poly(styrenesulfonate): a neutron reflectivity study.*

White Rose Research Online URL for this paper:  
<https://eprints.whiterose.ac.uk/144198/>

Version: Supplemental Material

---

**Article:**

Pérez, G.E., Bernardo, G., Gaspar, H. et al. (4 more authors) (2019) Determination of the thin film structure of zwitterion doped poly(3,4-ethylenedioxythiophene):poly(styrenesulfonate): a neutron reflectivity study. *ACS Applied Materials and Interfaces*, 11 (14). pp. 13803-13811. ISSN 1944-8244

<https://doi.org/10.1021/acsami.9b02700>

---

This document is the Accepted Manuscript version of a Published Work that appeared in final form in *ACS Applied Materials and Interfaces*, copyright © American Chemical Society after peer review and technical editing by the publisher. To access the final edited and published work see <https://doi.org/10.1021/acsami.9b02700>

**Reuse**

Items deposited in White Rose Research Online are protected by copyright, with all rights reserved unless indicated otherwise. They may be downloaded and/or printed for private study, or other acts as permitted by national copyright laws. The publisher or other rights holders may allow further reproduction and re-use of the full text version. This is indicated by the licence information on the White Rose Research Online record for the item.

**Takedown**

If you consider content in White Rose Research Online to be in breach of UK law, please notify us by emailing [eprints@whiterose.ac.uk](mailto:eprints@whiterose.ac.uk) including the URL of the record and the reason for the withdrawal request.



[eprints@whiterose.ac.uk](mailto:eprints@whiterose.ac.uk)  
<https://eprints.whiterose.ac.uk/>

Supporting Information

Determination of the Thin Film Structure of  
Zwitterion Doped Poly(3,4-  
ethylenedioxythiophene):Poly(styrenesulfonate).  
A Neutron Reflectivity Study

Gabriel E. Pérez,<sup>\*,†</sup> Gabriel Bernardo,<sup>‡</sup> Hugo Gaspar,<sup>‡</sup> Joshaniel F.K. Cooper,<sup>¶</sup>  
Francesco Bastianini,<sup>†</sup> Andrew J. Parnell,<sup>‡</sup> and Alan D.F. Dunbar<sup>\*,†</sup>

<sup>†</sup>*Department of Chemical and Biological Engineering, The University of Sheffield, S1 3JD,  
UK*

<sup>‡</sup>*Department of Physics and Astronomy, The University of Sheffield, S3 7RH, UK*

<sup>¶</sup>*ISIS Pulsed Neutron and Muon Source, STFC, Rutherford Appleton Laboratory, OX11  
0QX, UK*

E-mail: [geperez1@sheffield.ac.uk](mailto:geperez1@sheffield.ac.uk); [a.dunbar@sheffield.ac.uk](mailto:a.dunbar@sheffield.ac.uk)

Phone: +44 114 222 7555; +44 114 222 7551

# 1 Calculation of conductivity

The conductivity of the films was calculated using the following equation:

$$\rho = R_s \cdot t \tag{1}$$

$$\sigma = \frac{1}{\rho} \tag{2}$$

where  $\rho$  is the bulk resistivity,  $R_s$  is the sheet resistance,  $t$  is the film thickness, and  $\sigma$  is the film conductivity. The thickness (measured with ellipsometry) and sheet resistance measurements were performed immediately after annealing to minimize any swelling of the film due to ambient water absorption. A total of four sheet resistance measurements for each sample were taken (see table S1).

Table S1: *Sheet resistance and thickness values obtained for the pristine, 10, and 20 mM doped samples.*

Sample	$R_{s1}(\Omega/\square)$	$R_{s2}(\Omega/\square)$	$R_{s3}(\Omega/\square)$	$R_{s4}(\Omega/\square)$	$t(cm)$
Pristine	1.03E+07	9.24E+06	8.35E+06	8.79E+06	3.84E-06
10 mM	1.60E+07	1.37E+07	1.07E+07	1.68E+07	4.74E-06
20 mM	1.84E+05	1.21E+05	1.64E+05	7.87E+05	6.27E-06

# 2 Silicon oxide layer study

In order to corroborate that the first modeled layer (one above the Si substrate) is a true reflection of the substrate used for the pristine sample despite the unexpectedly thick SiO<sub>2</sub> layer, ellipsometry was conducted on the same sample that was measured with NR. This was done by removing the PEDOT:PSS from half the surface of the substrate with D.I. water and a cotton swab. Figure S1a shows the Psi and Delta values from the ellipsometry measurement along with their respective fits obtained by modelling a 5 nm thick oxidized layer on top of a Si layer. The relative similarity between the fits and the measured data suggests that the native oxide layer is  $\approx$  5 nm. To further corroborate that the 4.44 nm

layer determined by NR is a native oxide, atomic force microscopy (AFM) was conducted on the same cleaned substrate to obtain the roughness of the surface. The measured  $\sigma_{RMS}$  by AFM was  $0.92 \pm 0.05$  nm which is comparable to the 0.66 nm given by NR. In addition to this, the SLD of the NR fitted layer was  $3.17 \times 10^{-6} \text{ \AA}^{-2}$  which is in between the standard values for SiO ( $2.90 \times 10^{-6} \text{ \AA}^{-2}$ ) and SiO<sub>2</sub> ( $4.19 \times 10^{-6} \text{ \AA}^{-2}$ ). Given the previous evidence it is proposed that the layer on top of the silicon substrate is a slightly thicker than expected oxide layer. It is worth noting that this particular substrate came from a different batch of Si substrates, and was cleaned with a different process (using a H<sub>2</sub>O<sub>2</sub> solution) than the one described in the methodology section of the main manuscript.

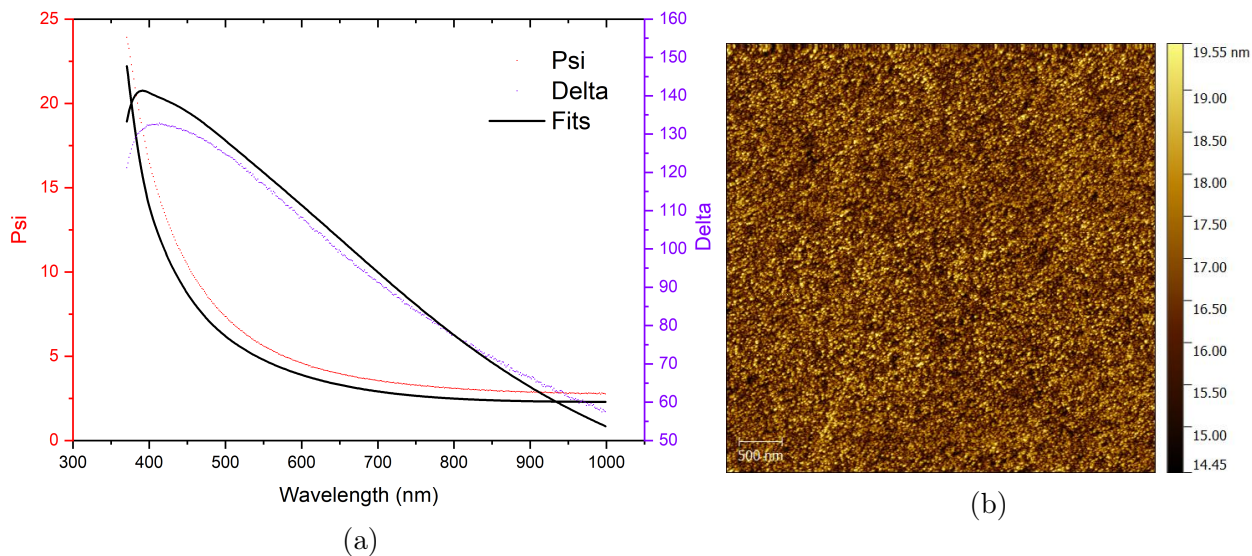


Figure S1: Ellipsometry data and fits (a) and AFM produced height image (b) for the SiO<sub>2</sub> layer.

### 3 Additional validation of the quality of the fit argument

In order to corroborate our findings in the neutron reflectivity section of this paper, we decided to further test the validity of our models by applying a two polymer layers model to the pristine sample and a three polymers layers model to the 10 mM sample. If the one layer model for the pristine sample had a  $\chi^2$  very similar to the one of the two layer model then we could confirm that the one layer model describes correctly the pristine film structure.

Moreover, if the three layer model for the 10 mM sample has a  $\chi^2$  very similar to the two layer model then we can corroborate that the two layer model correctly describes the film structure as well. The results can be seen in figure S2.

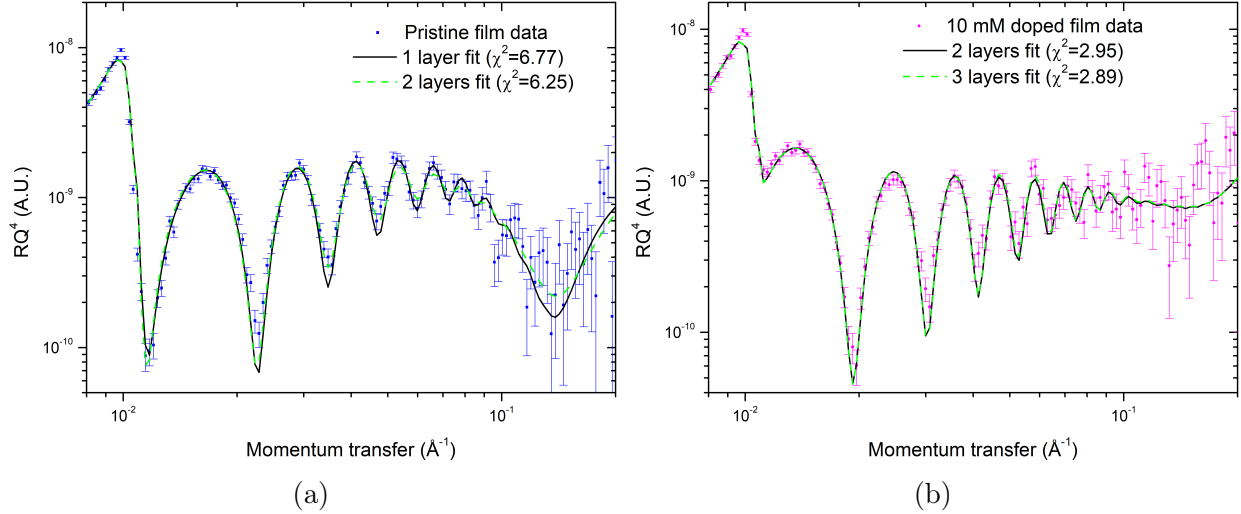


Figure S2: Neutron reflectivity plotted as  $RQ^4$  data for (a) the pristine film and its corresponding fits using a one layer model (black line), a two layer model (green spaced line), and for (b) the 10 mM film and its corresponding fits using a two layer model (black line) and a three layer model (green spaced line) both under the same simulation conditions. The  $\chi^2$  values of each fit are shown for comparison of quality of the fits.

Table S2: Thickness ( $D$ ), root mean square roughness ( $\sigma_{RMS}$ ), and scattering length density ( $SLD$ ) resulting from modelling a 2 layer and 3 layer model for the pristine and 10 mM sample respectively.

Pristine (2 layer model)			
	D (nm)	$\sigma_{RMS}$ (nm)	SLD ( $10^{-6}\text{\AA}^{-2}$ )
Top Layer	39.78	2.43	1.5
Bottom Layer	8.51	4.94	1.28
10 mM (3 layer model)			
	D (nm)	$\sigma_{RMS}$ (nm)	SLD ( $10^{-6}\text{\AA}^{-2}$ )
Top Layer	43.6	1.16	1.37
Middle Layer	2.13	1.91	1.47
Bottom Layer	10.1	6.48	1.07

As it can be appreciated in figure S2a, the  $\chi^2$  values of one layer and two layer models for the pristine sample are 6.77 and 6.25 respectively, which are very similar (7.7% improvement of the quality of the fit from the one layer model to the two layer model). This implies that the one layer model is the best interpretation for this film structure. Figure S2b shows as

well two similar  $\chi^2$  values from the three layers (2.95) and two layers (2.89) model for the 10 mM sample (2.1% increase from the two layer model to the three layer model) indicating that, based on the Occam's Razor's principle,<sup>1</sup> the two layer model is the best interpretation for this film structure.

## 4 Beyond the chi squared analysis of the models

To further confirm our findings, we performed an additional analysis for all the models presented in this work based on the following considerations:

1. Free fitting all the parameters of the system (i.e. SiO<sub>2</sub>, PEDOT:PSS and additional layers).
2. Fitting the system with the SiO<sub>2</sub> layer highly constrained to represent consistency across the different wafers.
3. Fitting the systems with n+1 layers of PEDOT:PSS, where n is the number of layers which gives the best fit.

The analysis of the fits were based on the following considerations:

1. The goodness of the fit, which is represented by the probabilistic evidence.
2. The change in SLD and the data's sensitivity to it.
3. Improvement of the fit over a simpler model

All of the fits were constrained to the Nevot Croce theory,<sup>2</sup> so roughness could not be more than half the layer thickness, and no sharp transitions were allowed. Fits were stopped when the models were stable to perturbation, i.e. obtain a fit, then change one of the parameters then refit and the same solution is achieved. The normalisation constant used was a log with error-bar based figure of merit (described in GenX help) as this gave

greater sensitivity across the range of Q. The reflectivity curves are all of high enough quality to resolve the differences we are looking at.

## 4.1 Native oxide layer

This was set for all wafers to be around 40 Å thick, with an SLD around  $3.5 \times 10^{-6} \text{ \AA}^{-2}$ .

## 4.2 Pristine PEDOT:PSS

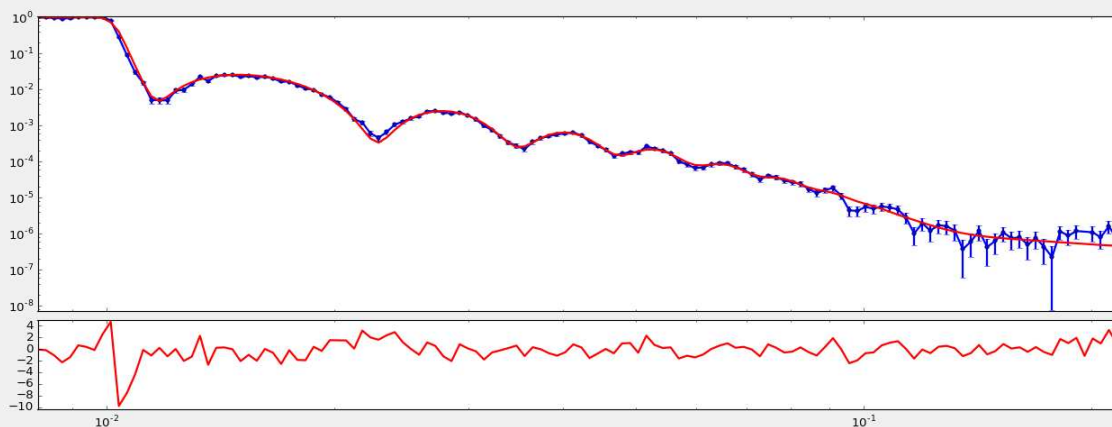
Table S3: *Figure of merit (FOM), scattering length densities (SLD's) and total thickness resulting from 1 layer and 2 layer models for the pristine sample.*

Pristine PEDOT:PSS		
	1 layer	2 layers
FOM	1.65	1.648
SLD 1 ( $10^{-6} \text{ \AA}^{-2}$ )	1.399	1.4
SLD 2 ( $10^{-6} \text{ \AA}^{-2}$ )	-	1.399
Total thickness (Å)	481	481

As shown in table S3 , and figures S3 and S4 the data is clearly described as well as it could be using a single PEDOT-PSS layer. The SLD and fit curves both look almost identical for the 1 and 2 layer models.

FOM logbars: 1.1650e+00

### Pristine, 1 layer



Data FOM Pars FOM scans SLD

	Parameter	Value	Fit	Min	Max	Error
-	inst.setIbkg	4e-07	<input type="checkbox"/>	1e-08	1e-05	-
-		0	<input type="checkbox"/>	0	0	0
0	Sub.setSigma	12.16374	<input checked="" type="checkbox"/>	2	20	20
-		0	<input type="checkbox"/>	0	0	0
1	SiO2.setD	43.21388	<input checked="" type="checkbox"/>	10	60	60
-	SiO2.setSigma	6	<input type="checkbox"/>	5	15	15
2	SiO2.setSld_nreal	3.382545	<input checked="" type="checkbox"/>	0.5	5	5
-		0	<input type="checkbox"/>	0	0	0
3	PEDOT_PSS.setD	481.62	<input checked="" type="checkbox"/>	300	600	600
4	PEDOT_PSS.setSigma	24.73316	<input checked="" type="checkbox"/>	5	25	25
5	PEDOT_PSS.setSld_nreal	1.399184	<input checked="" type="checkbox"/>	-5	5	5
-			<input type="checkbox"/>			

Grid Script Sample Simulations

Simulation Successful xy

Figure S3: Neutron reflectivity data, fit, and fitting parameters for the 1 layer model of the pristine sample in GenX.

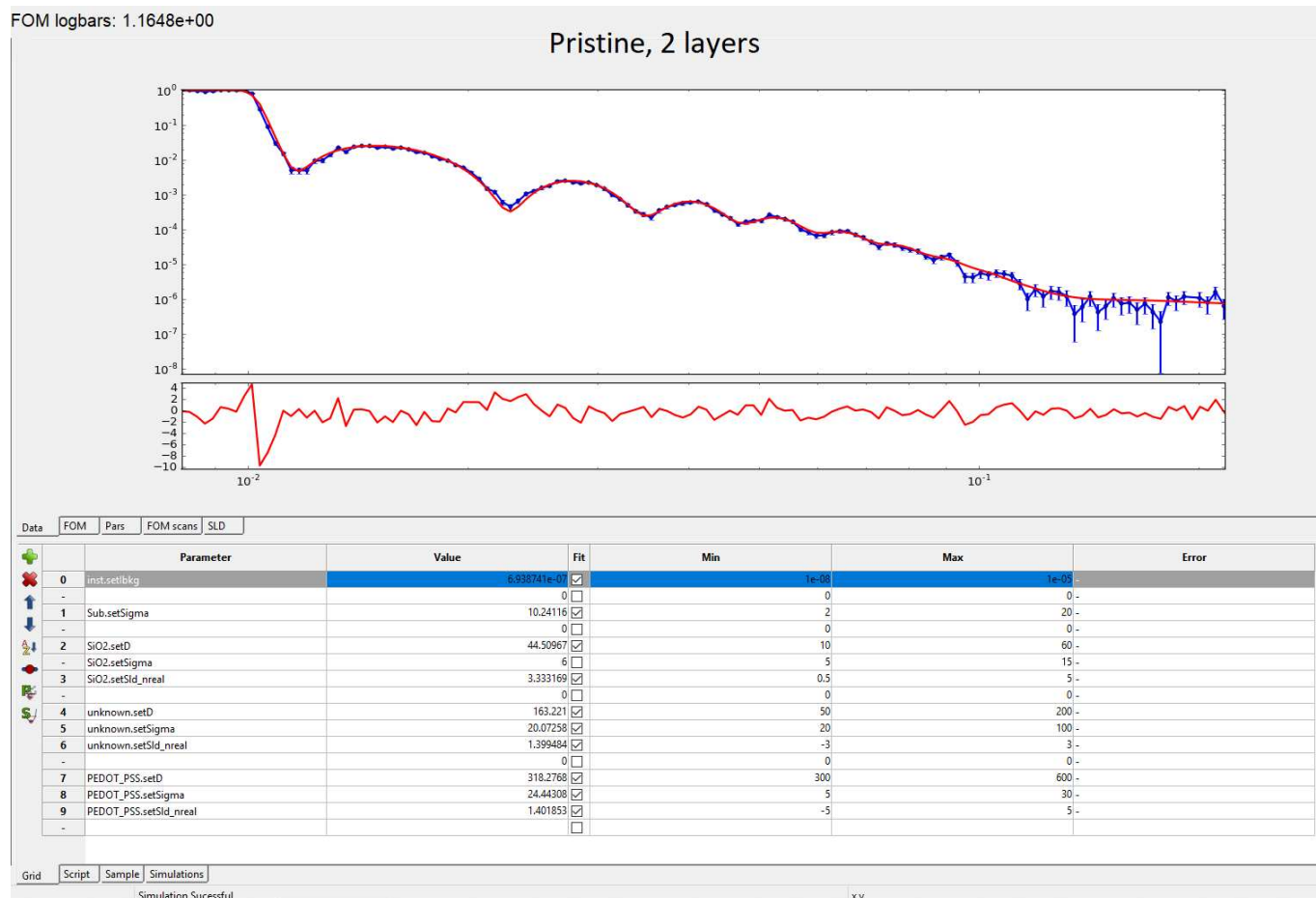


Figure S4: Neutron reflectivity data, fit, and fitting parameters for the 2 layer model of the pristine sample in GenX.

### 4.3 10 mM DYMAP doped PEDOT:PSS

Table S4: Figure of merit (FOM), scattering length densities (SLD's) and total thickness resulting from 1 layer, 2 layers, and 3 layer models for the 10 mM sample.

10 mM DYMAP doped PEDOT:PSS			
	1 layer	2 layers	3 layers
FOM	1.28	1.10	1.10
SLD 1 ( $10^{-6} \text{ \AA}^{-2}$ )	1.16	1.11	1.11
SLD 2 ( $10^{-6} \text{ \AA}^{-2}$ )	-	1.24	1.18
SLD 3 ( $10^{-6} \text{ \AA}^{-2}$ )	-	-	1.24
Total thickness ( $\text{\AA}$ )	554	554	554

As shown in table S4 and figures S5, S6, and S7 the fit here is improved both by the

metric of FOM, and visually, by the splitting of the PEDOT:PSS into two distinct layers. Adding a third layer to the system does not improve the FOM, but interestingly does seem to reproduce the SLD of the 2 layer model, suggesting a stable minima in the fit.

Compared to the pristine film, this film (10 mM) is thicker and has a lower SLD. The preparation of the films was identical in the procedure, but the addition of the DYMAP does increase the viscosity of the solution, thus a thicker film is expected. In addition, since DYMAP causes the films to swell in this system, it is also likely to have changed the SLD of the film. Since the combination of increased viscosity and swelling can both have the same effect, we cannot easily disentangle each's contribution.

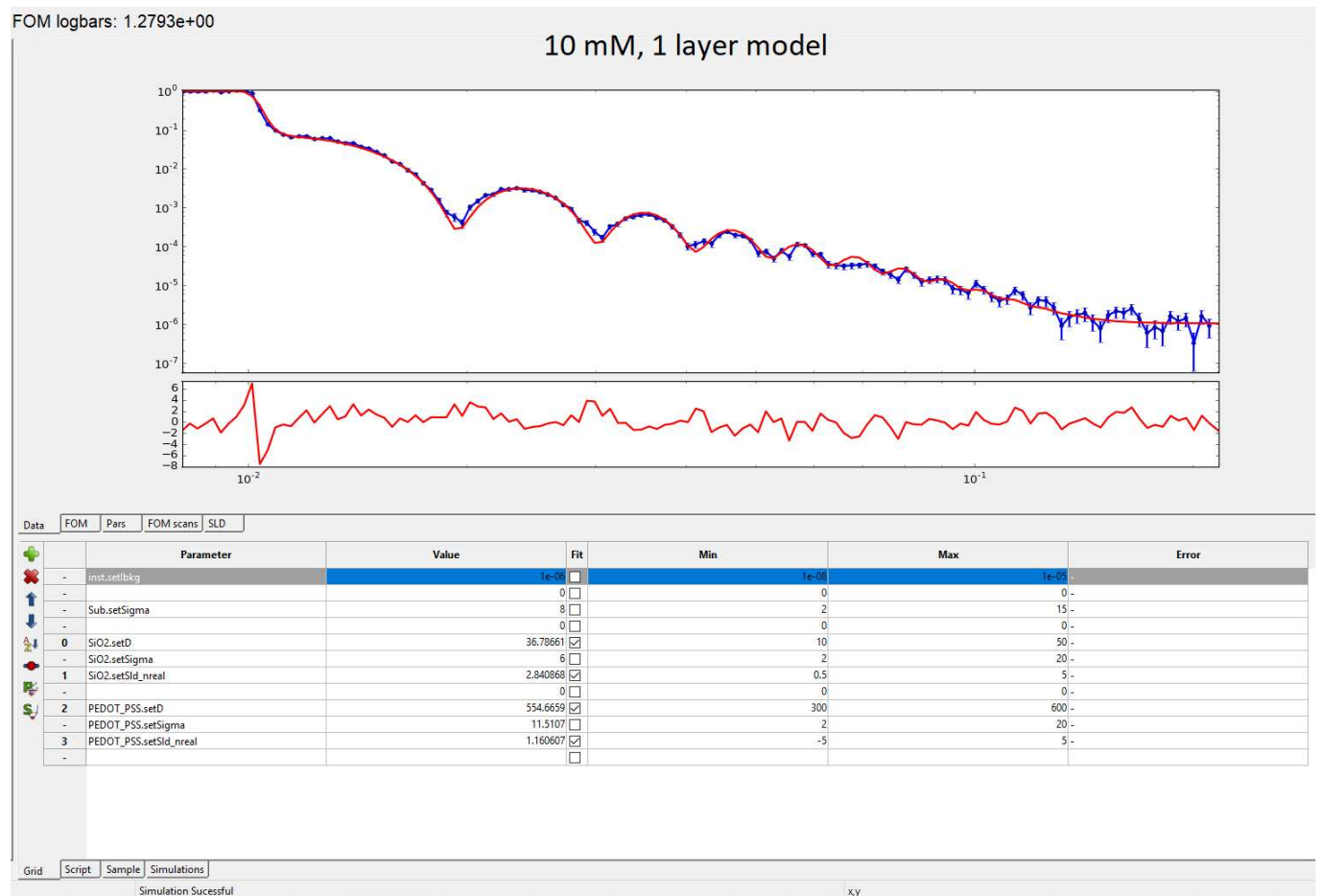


Figure S5: Neutron reflectivity data, fit, and fitting parameters for the 1 layer model of the 10 mM sample in GenX.

FOM logbars: 1.1021e+00

### 10 mM, 2 layer model

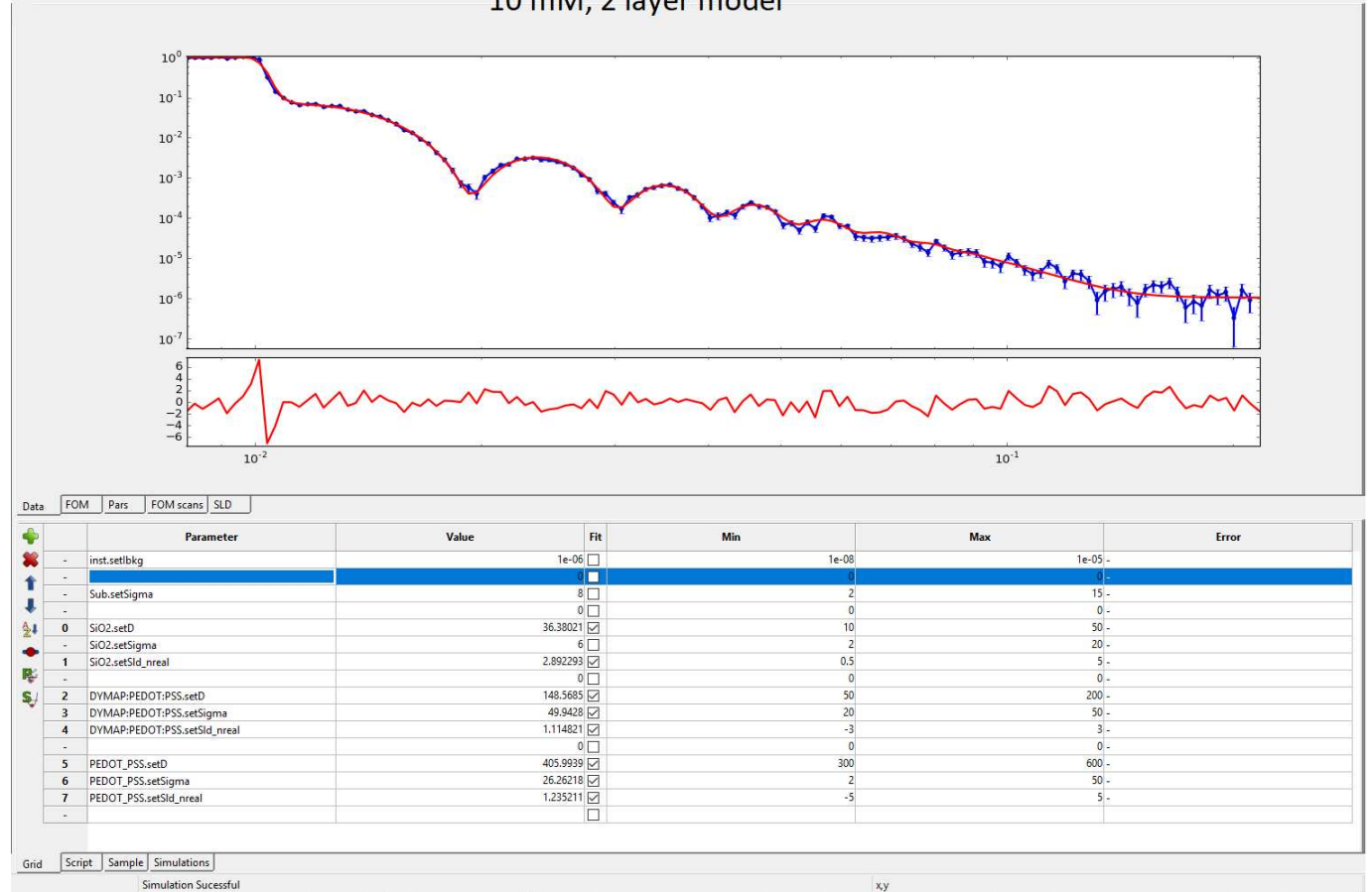


Figure S6: Neutron reflectivity data, fit, and fitting parameters for the 1 layer and 2 layer models of the 10 mM sample in GenX.

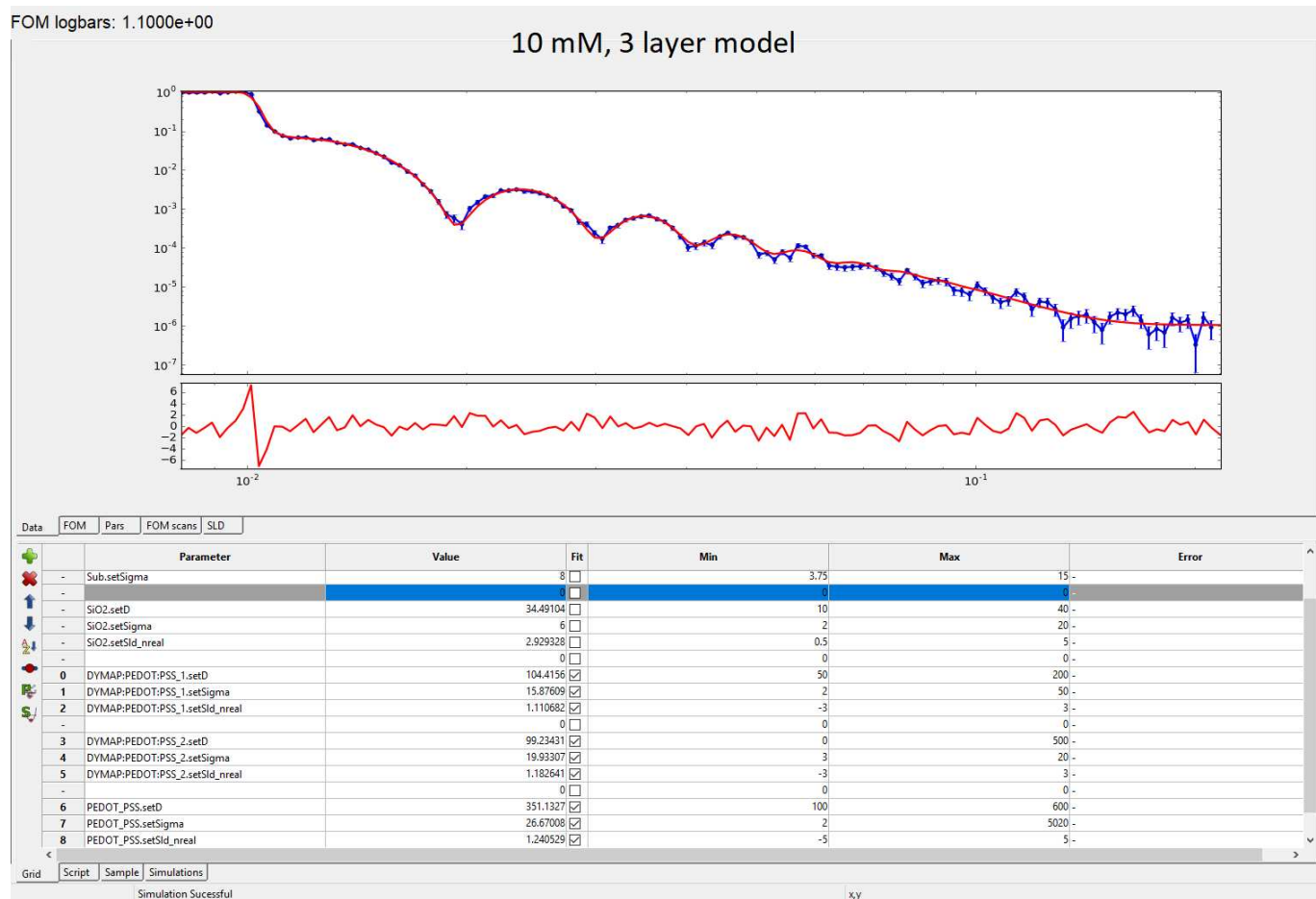


Figure S7: Neutron reflectivity data, fit, and fitting parameters for the 1 layer, 2 layers, and 3 layer models of the 10 mM sample in GenX.

#### 4.4 20 mM DYMAP doped PEDOT:PSS

Table S5: Figure of merit (FOM), scattering length densities (SLD's) and total thickness resulting from 1 layer, 2 layers, and 3 layer models for the 10 mM sample.

20 mM DYMAP doped PEDOT:PSS			
	1 layer	2 layers	3 layers
FOM	1.03	0.99	0.95
SLD 1 ( $10^{-6} \text{ \AA}^{-2}$ )	0.81	0.69	1.08
SLD 2 ( $10^{-6} \text{ \AA}^{-2}$ )	-	0.87	0.82
SLD 3 ( $10^{-6} \text{ \AA}^{-2}$ )	-	-	1.18
Total thickness ( $\text{ \AA}$ )	771	791	778

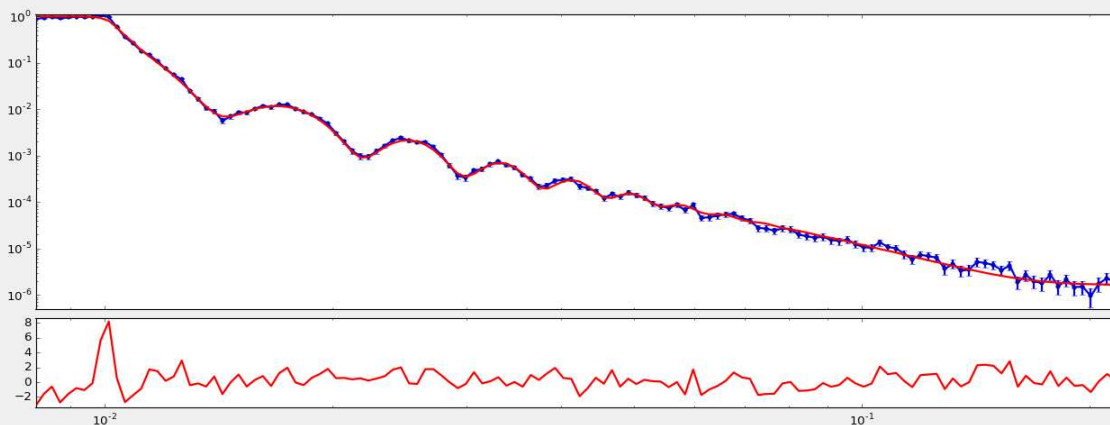
As shown by table S5 and figures S8, S9, and S10 the changes in FOM elicited by the

increase in layers are less clear cut in this sample. The SLDs of the films are again reduced with respect to the undoped sample, and the thickness again increased. As discussed for the 10mM sample, this is not unexpected, nor easily analysed further.

The SLD change for the two layer structure is less than half that of the 10mM sample and possibly pushing the limits of what sort of change would be detectable for an NR experiment. A similar size of SLD change is seen in the three layer model. In the three layer and two layer models we see that for the first time, the total thickness does not agree across the three fits. This is possibly due to the fact that the top layer of the such models is a change to the top interface, making a previously rough looking interface into almost a step function. Since the fits and the FOM's are nearly identical, we can say that we do not have the ability to distinguish between the two models. However, Occam's razor<sup>1</sup> would suggest to take a model with less parameters and a similar goodness of fit. Overall, the 20 mM sample's models with additional layers do not improve the agreement with the data enough to justify their inclusion. If any additional layers might be present, the SLD's would suggest a slightly lower SLD layer nearer the Si surface, in the same manner that we saw with the 10mM film. However, to conclude this would not be reasonable given the experimental data. Therefore we conclude that this film is best described by a single layer model.

FOM logbars: 1.0267e+00

### 20mM, 1 layer model



Data							
FOM		Pars	FOM scans	SLD			
Parameter	Value	Fit	Min	Max	Error		
- inst.setibkg	1.5e-08	<input type="checkbox"/>	1e-08				
-	0	<input type="checkbox"/>	0				
0 SiO2.setD	31.53411	<input checked="" type="checkbox"/>	20		50 -		
1 SiO2.setSigma	2.001341	<input checked="" type="checkbox"/>	2		20 -		
2 SiO2.setSld_nreal	2.762075	<input checked="" type="checkbox"/>	2		6 -		
-	0	<input type="checkbox"/>	0		0 -		
3 PEDOT_PSS.setD	770.6363	<input checked="" type="checkbox"/>	300		800 -		
4 PEDOT_PSS.setSigma	17.07241	<input checked="" type="checkbox"/>	2		50 -		
5 PEDOT_PSS.setSld_nreal	0.8074676	<input checked="" type="checkbox"/>	0		2 -		
-		<input type="checkbox"/>					

Figure S8: Neutron reflectivity data, fit, and fitting parameters for the 1 layer model of the 20mM sample in GenX.

FOM logbars: 9.8819e-01

### 20 mM, 2 layer model

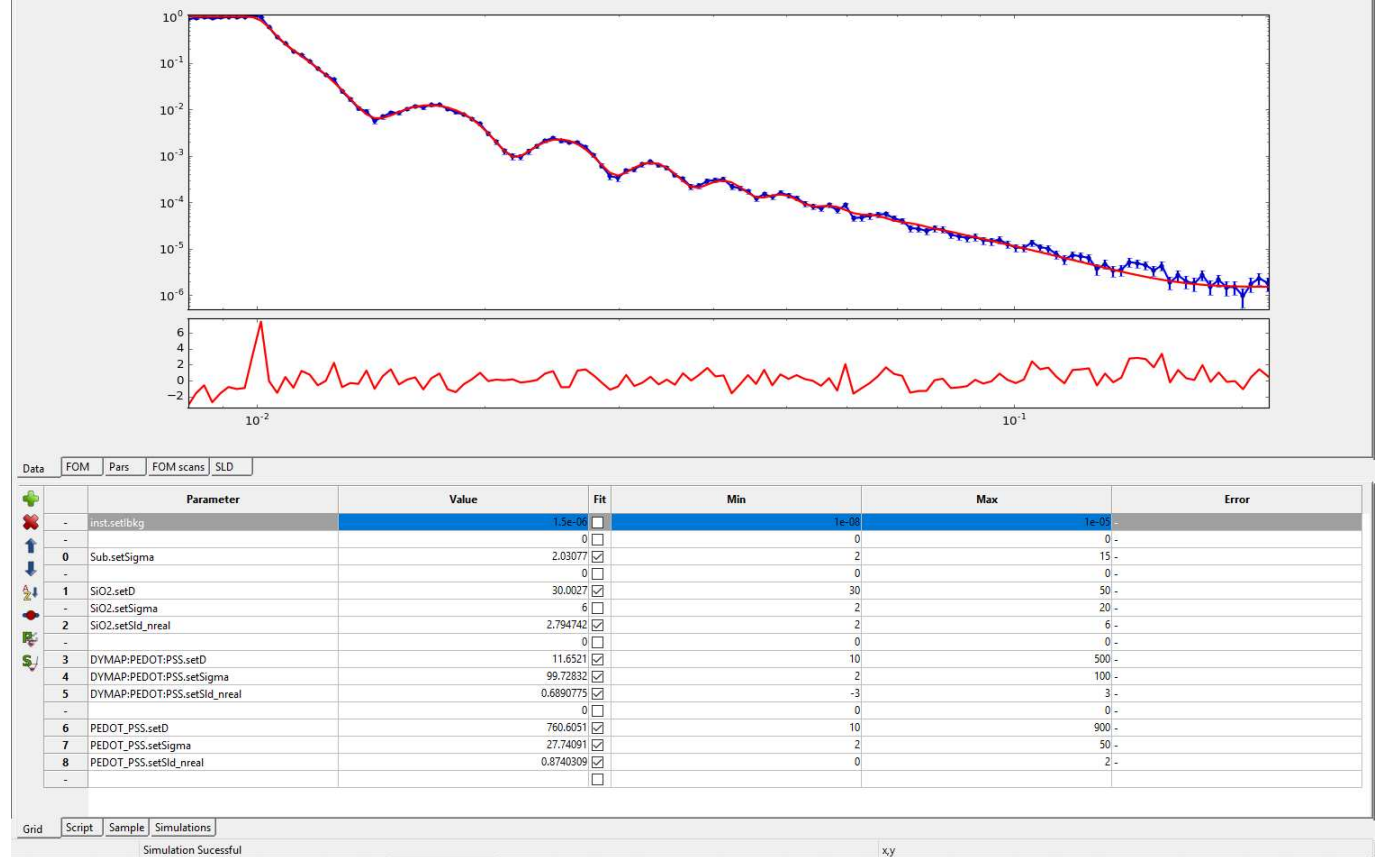


Figure S9: Neutron reflectivity data, fit, and fitting parameters for the 2 layer model of the 20 mM sample in GenX.

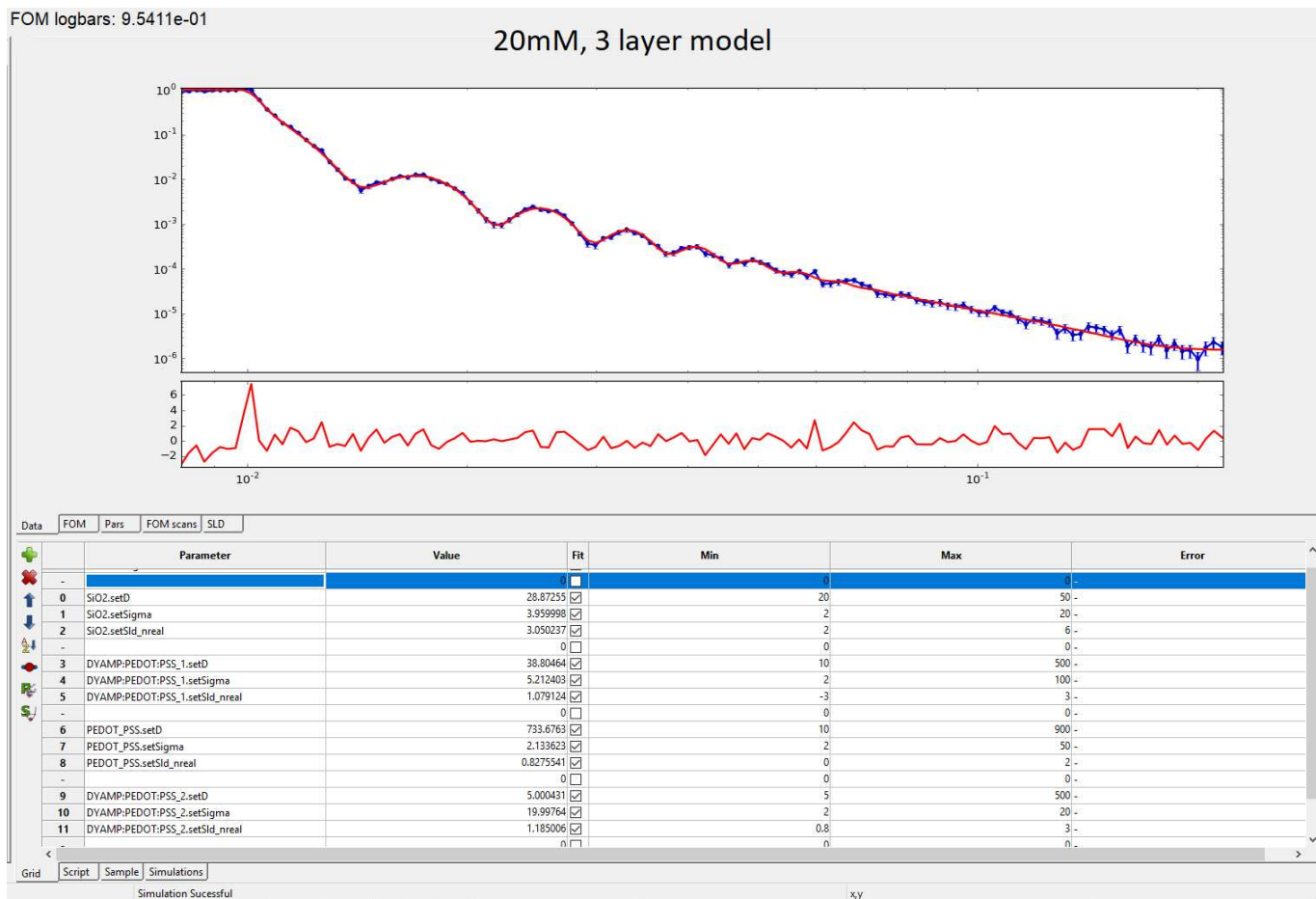


Figure S10: Neutron reflectivity data, fit, and fitting parameters for the 3 layer model of the 20 mM sample in GenX.

## 5 Device performance

The photovoltaic performance of devices fabricated with pristine, 10 mM, and 20 mM doped PEDOT:PSS as a HTL is shown in figure S11.

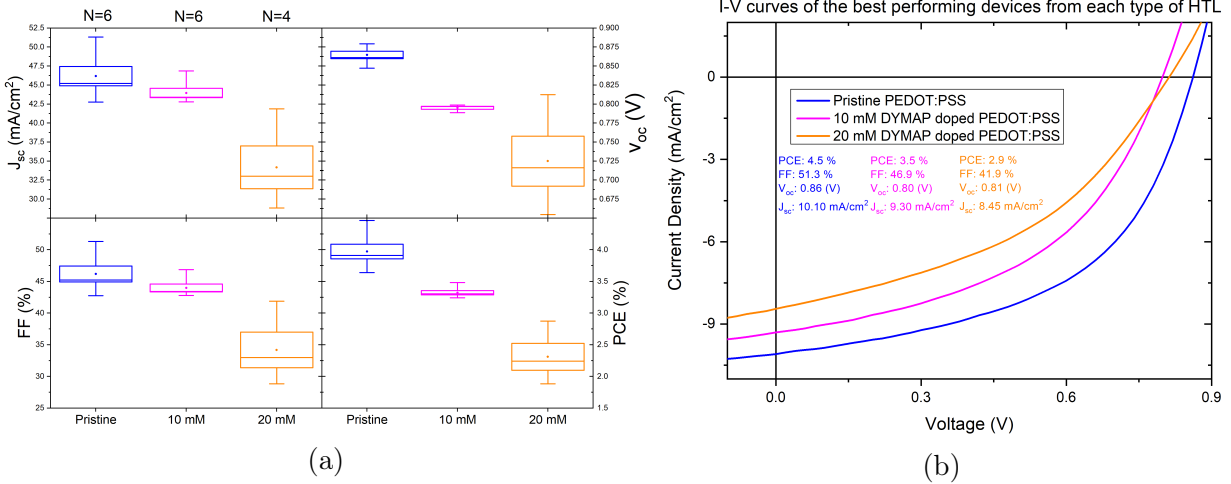


Figure S11: (a) Photovoltaic performance of PCDTBT:PC<sub>71</sub>BM based devices with pristine, 10 mM, and 20 mM DYMAP doped PEDOT:PSS used as the HTL.  $N$  equals number of devices measured, the height of the box represents the standard error, the top and bottom ticks are the maximum and minimum value, the horizontal line in the box is the median, and the circle in the middle of the box is the mean average value. (b) I-V curve and photovoltaic parameters of the best performing pixel for each type of device fabricated.

We were expecting to see an increase in the power conversion efficiency (PCE) of the 20 mM sample since its conductivity is significantly increased by more than one order of magnitude compared to the pristine and the 10 mM sample. However not only the overall PCE of the devices went down from 4.5% to 3.5% and 2.9% as the concentration of DYMAP increased, but also all the other photovoltaic parameters decreased as it can be appreciated in figure S11a. Moreover the I-V curves (figure S11b) of the best performing devices for each HTL show a clear detriment in the quality of the devices as a function of the doping concentration. We attribute these trends to the quality of the contact between the active layer and the different hole transporting layers. During the spin coating step of the fabrication process the doped films demonstrated an increased phobic behaviour towards the solvent (chlorobenzene) in which the active layer was diluted. This resulted in difficulties spin-coating the active layer onto the doped PEDOT:PSS films evidenced by areas on the HTL layer that were not coated due to the surface repelling the active layer solution. This effect was considerably more intense, and hence more evident in the 20 mM doped sample compared to the 10 mM doped one which explains the wider error bars of the 20 mM data in figure

S11a. In order to corroborate that the doped samples exhibit a phobic behaviour towards chlorobenzene, we conducted contact angle measurements on the pristine, 10 mM, and 20 mM doped samples by dropping 5  $\mu\text{L}$  of chlorobenzene on the surface of each sample. As shown in figure S12 the contact angle increases from  $10.58^\circ$  to  $16.15^\circ$  from the pristine to the 10 mM doped sample respectively confirming and increased phobic behaviour of the doped sample towards chlorobenzene. This phobic behaviour was found to have a correlation with the doping concentration since the contact angle of the 20 mM doped sample was  $20.48^\circ$ . These results confirmed that the doped samples develop a phobic behaviour towards the active layer solvent. The increased phobic behaviour of the DYMAP doped PEDOT:PSS film hinders the quality of the contact between the HTL and the active layer due to the increased dewetting. This slightly increases the series resistance of the devices and most prominently decreases their shunt resistance (as shown by the shape of the I-V curves in figure S11b) allowing for a leakage current to hinder the photovoltaic parameters and performance of the solar cells using DYMAP doped PEDOT:PSS. It is worth mentioning that the champion 10 mM and 20 mM devices had an almost identical open circuit voltage ( $V_{oc}$ ) which is definitely lower than that one of the undoped sample. This indicates that the HOMO and LUMO levels of the HTL film may be shifted by the inclusion of DYMAP in PEDOT:PSS modifying its electron blocking capabilities. This could lead to more recombination events within the device and hence a poor performance. For future work in device fabrication with DYMAP doped PEDOT:PSS as an HTL we suggest investigating an improved methodology to enhance the contact between the doped HTL films and the active layer. Additionally we recommend a study on the energy levels dependence of DYMAP doped PEDOT:PSS films as a function of the dopant concentration and their electron blocking capabilities.

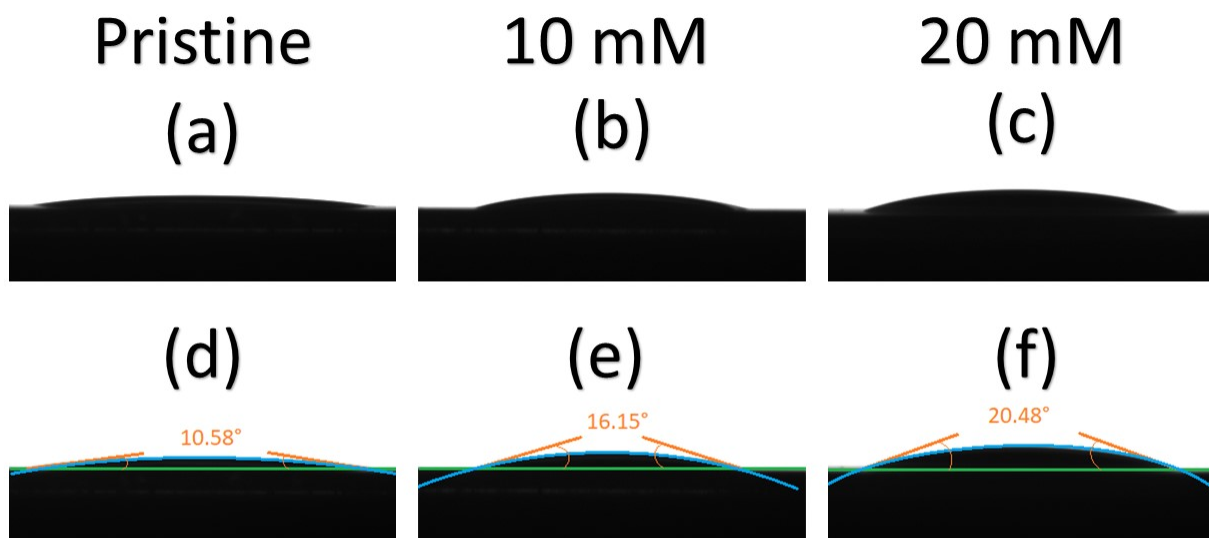


Figure S12: Contact angle images of the pristine (a and d), 10 mM (b and d), and 20 mM (c and f) DYMAP doped samples. 5  $\mu$ L of chlorobenzene were dropped on top of the films for these measurements.

## References

- (1) Walsh, D. Occam's razor: A Principle of Intellectual Elegance. *Am. Philos. Q.* **1979**, *16*, 241–244.
- (2) Nevot, L.; Croce, P. Caractérisation des Surfaces par Réflexion Rasante de Rayons X. Application à l'étude du Polissage de Quelques Verres Silicates. *Rev. Phys. Appl.* **1980**, *15*, 761–779.